Parameters Influencing Fluid Particle Interactions in Anatomical Flows: A Review

Afnan Al-haj [*1], John Boddu [†1], and Akshita Sahni [‡1]

[1]Dept. of Mechanical Engineering, University of Colorado at Boulder

Abstract

Finite-sized (or inertial) particles in fluid flow do not follow the flow trajectory and are known to have non-trivial transport characteristics controlled by the particle's shape, size, and intrinsic activity. Fragmented clot particles(embolus) can travel across human arteries, causing a blockage of cerebral artery and disrupt blood supply to a region of the brain. This is the mechanism of embolic stroke- a disease contributing to the second leading cause of death and a leading cause of disability worldwide. The heart, arteries, and veins constitute the human circulatory system, which transports blood to the various organs of the human body. Numerous functional and anatomical features are at interplay in this transport system. The tubular vessels (arteries and veins) are flexible, curved, and display a complex branching system thereby adding a three-dimensionality to the blood flow. Blood is a complex fluid due to the cellular and nutrient constitution; its viscous properties vary with flow shear rates. Thus, it can be inferred that the prediction of particle transport through blood vessels is a challenge due to the multitude of parameters at interplay within such a dynamic circulatory system. This review paper aims at describing a number of computational studies and one experimental study conducted to characterise embolus transport through the human vasculature.

Keywords: embolus; elastohydrodynamic contact; one-way coupling; Maxey-Riley equation; Navier-Stokes equation

[*]afal9297@colorado.edu
[†]john.boddu@colorado.edu
[‡]akshita.sahni@colorado.edu

1 Introduction

Disturbed flow in arteries is believed to be one of the most important causes of cardiovascular diseases. The aorta, being the largest artery, is especially prone to illness [2], and around 36% of strokes are caused by emboli [1]. The fact that emboli (fragmented clots and calcifications) in the bloodstream should generally favor arteries that receive the highest volumetric blood flow might only be intuitively accurate. An accurate description of distribution of emboli accounts for the unique fluid dynamics which requires a complete framework to account for anatomical variations of the artery and the embolus interaction with the vessel walls. Therefore, the major objective of this review is focused on studies investigating the propensity of embolic particles to be transported to various branches downstream of the flow and the size-dependent predilections of this transport. Thus, our study seeks to understand:

• An accurate description of the boundary conditions to solve particle transport equations

• Particle transport dynamics using modified Maxey-Riley equation to account for embolus-wall interactions and fluid particle two way coupled interactions

• The role of anatomical variations(which lead to flow structures) in affecting embolus distribution across the arteries.

2 Modeling

2.1 Image-based CFD framework

Three-dimensional (3D) models of the selected vasculature segments were used for the computational modeling of the flow. These models were derived from patient Computed Tomography (CT) scan data by reconstructing blood vessel lumen of the chosen vasculature segment and translating it into 3D computer models using SimVascular software [1] and ITK-SNAP image processing packages [6] based on active contour techniques. This process is depicted in Figure 1. The aortic arch typically possesses the most complex flow structures and plays a key role in determining whether the emboli are directed towards the head or the rest of the body. Thus the models utilized in the discussed studies comprised of 1) aortic arch with descending aorta and the branch arteries (referred to as the 'aorto-femoral model') or 2) aortic arch with superior arch vessels leading to the circle of Willis in the brain (referred to as the 'aorto-cerebral model') [7]. Carr *et al.* studied the influence of anatomical variations in biasing the embolus transport at the level of the aortic arch and first-generation branches to the head. Therefore, their distinct models from multiple patient geometries were truncated at the level of the common carotid and vertebral arteries.

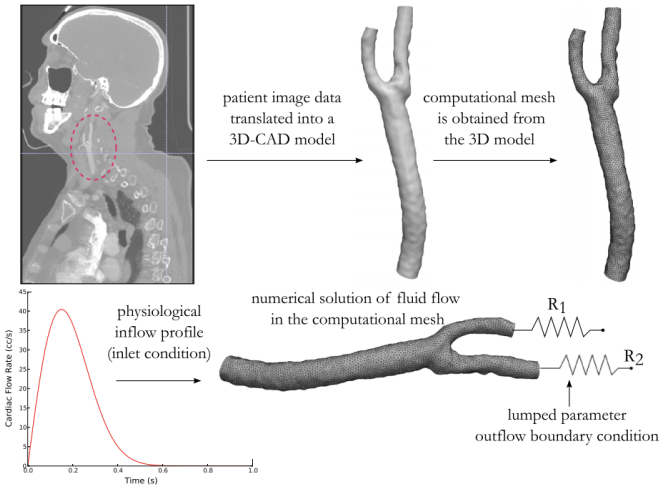

Figure 1: A schematic description shows the overall CFD framework of a patient-specific based simulation. This photo was reproduced with the permission of Mukherjee. *et al.* [6].

On the other hand, Mukherjee *et al.* [6, 7] studied embolus transport to the brain by varying embolus properties and release mechanisms; they used patient aortic arch geometries free of pre-existent anatomical features to better isolate influence of embolus properties [5]. In another study comparing the fluid-structure interactions with the emboli, Mukherjee *et al.* utilized an idealized Y-bifurcation model and an anatomical model of the carotid artery from one patient to assess the influence of vortical flow in the idealized versus anatomical geometries. The model domains were discretized into computational meshes comprising tetrahedral elements. Blood was assumed to be a Newtonian fluid with constant density 1025 kg/m^3, and dynamic viscosity 0.004 Pa·s. A specific physiologic volumetric flow waveform (as defined by Olufsen [8]) was prescribed at the inlet boundaries of the 3D models of the respective vasculature segments used the described studies.

2.2 Boundary flow conditions and flow-solver

In the study conducted by Vignon-Clementel *et al.* [10], blood flow in large arteries was found to be largely dependent on the outflow boundary conditions assigned to the downstream vascular beds of the 3D computational domain. Thus, the assignment of appropriate boundary conditions is one of the important factors in analyzing particle transport in anatomical flows. The critique of commonly prescribing constant pressure or traction is that this oversimplification leads to inaccurate predictions of velocity and pressure fields where the flow distribution and pressure field in the modeled domain are unknown. The alternative suggested by the authors is to couple the solution at the outflow boundaries using lumped resistors to account for the flow resistance from the downstream domain. The capability of this method is presented in three separate works of Mukherjee *et al.* [4, 6, 7] in the context of a Petrov-Galerkin stabilized linear finite-element method.

$$\rho_f(\frac{\partial \mathbf{u}}{\partial t} + (\mathbf{u}\cdot\boldsymbol{\nabla}\mathbf{u})) = -\boldsymbol{\nabla}p + \boldsymbol{\nabla}\cdot\boldsymbol{\tau} + \rho_f\mathbf{g} \tag{1}$$

$$\boldsymbol{\nabla}\cdot\boldsymbol{u} = 0 \tag{2}$$

$$\tau = 2\mu_f\mathbf{D(u)} = \mu_f(\boldsymbol{\nabla}\boldsymbol{u} + \boldsymbol{\nabla}\boldsymbol{u}^T) \tag{3}$$

Eq. (4) describes the complete, generalized variational form of the combined Navier-Stokes (1), continuity (2), and constitutive stress-strain laws for Newtonian fluids (3) equations.

$$\rho_f(\mathbf{w}, \frac{\partial \mathbf{u}}{\partial t})_\Omega + \rho_f(\mathbf{w}, (\mathbf{u}\cdot\boldsymbol{\nabla})\mathbf{u})_\Omega + 2\mu_f(\mathbf{D}(\mathbf{u}), \mathbf{D}(\mathbf{u}))_\Omega - \rho_f(\mathbf{w}, \mathbf{b})_\Omega - (\boldsymbol{\nabla}\cdot\mathbf{w}, p)_\Omega - (\boldsymbol{\nabla}q, \mathbf{u})_\Omega + (q, \mathbf{u}\cdot\mathbf{n})_\Gamma$$
$$- \underbrace{(\mathbf{w}, \mathbf{h})_{\Gamma_t \ominus \Gamma_B}}_{Traction\ Boundaries} + \underbrace{(\mathbf{w}, \mathbf{h}_{0D})_{\Gamma_B}}_{Outflow\ Boundaries} + \sum_{e=1}^{N_{el}} \left[\underbrace{(\tau_{supg}(\mathbf{u}^h\cdot\boldsymbol{\nabla})\mathbf{w}^h, \mathcal{R}^h)_{\Omega,e}}_{SUPG\ Stabilization} + \underbrace{(\tau_{pspg}\boldsymbol{\nabla}q^h, \mathcal{R}^h)_{\Omega,e}}_{PSPG\ Stabilization} \right] = 0 \tag{4}$$

In Eqs. (1)-(4), density is denoted by ρ_f, $\mathbf{g}$ denotes gravity; $\mathbf{u}$, p denote the blood flow velocity and pressure; $\mathbf{w}$, $\mathbf{q}$ denote the finite element test functions, μ_f is the blood viscosity, Ω indicates the overall computational domain encompassing the upstream and downstream vasculature, Γ and its subscripts indicate the various coupling boundaries, R_h denotes the residual of the momentum equation, and $\tau_{supg/pspg}$ are stabilization parameters for convective flow and pressure stability using equal order finite elements respectively.

2.2.1 Resistance boundary condition

Considering the domain, appropriate boundary flow conditions are selected [4, 5]: an average volumetric inflow at the aorta inlet based on magnetic resonance (MR) measurements was kept consistent at 79 mL/s across each of the anatomical models, and resistance based boundary conditions were assigned to account for flow resistance from downstream vascular beds. The importance of coupling the outlet pressure with the computed outlet flow rate at the outlet boundaries is the explicit relationship of pressure as a function of flow rate or velocities that are obtained at the coupling interface. To estimate resistance values at each

outlet, the average flow distribution to each outlet is assumed proportional to cross-sectional areas of the respective outlet, i.e $Q_i \propto A_i$ [1, 5, 6, 7]. Distinct outflow boundary conditions using resistive and/or capacitive models were coupled to the 3D computational domain to represent the respective downstream vascular bed. Carr *et al.* [1] used single element Windkessel models, the resistance of which was set to produce an expected mean flow rate to each arterial bed. Based on mean aortic flow distribution measurements, 65% of the flow was nominally distributed to the aorta, and the remaining 35% distributed according to vessel area to aortic arch branch arteries [1]. Subsequently, the resistance at each outlet was set according to $R_e = \frac{\overline{P}}{\overline{Q}}$. Mean brachial pressure was used for $\overline{P}$. For the aorto-cerebral model, lumped resistor outflow boundary conditions were employed, with resistor values for the six major cerebral arteries tuned to achieve average flow rates from measured MR data. For the aorto-femoral model, three-element Windkessel outflow boundary conditions were employed, with all resistance and capacitance values estimated based on assumed target flow division across all outlets [7].

To emphasize the importance of implementing appropriate boundary conditions, Vignon *et al.* performed numerical simulations of an abdominal aorta bifurcation to the iliac arteries with a 75% area reduction stenosis on the right. In Figure 2, the constant pressure boundary condition has flow to the normal iliac artery exceeding that to the stenosed for all points in time. For the impedance boundary condition, the peak flow is greater in the normal iliac artery, whereas during late systole and early diastole, the flow is greater in the stenosed iliac artery. A pulsatile, parabolic flow profile was assigned at the inlet, and constant pressure was prescribed at the two outlets. The constant outlet pressure imposes a limitation on the split of the flow, and it is characterized by the sheer resistance to flow due to the geometry of the computational domain. In contrast, an impedance boundary condition allows the downstream conditions to determine the flow split [10]. The appropriate framework for patient-specific modeling, followed by the limitations and opportunities to improve cardiovascular flow modeling were analyzed. Blood flow velocity and pressure fields were obtained by utilising finite element methods (FEM) [7], using the SimVascular software package (Updegrove *et al.*, 2016 [9]) FEM is well suited for cardiovascular simulation, since an unstructured discretization can be used to accurately model complex vascular geometries [1].

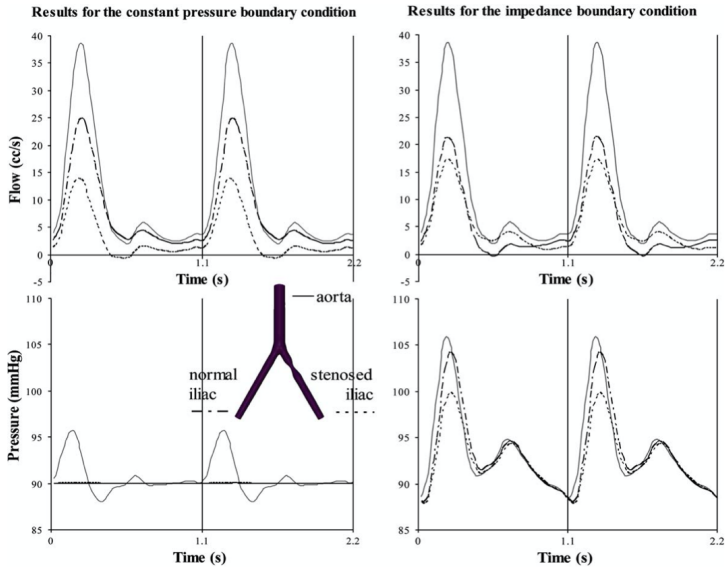

Figure 2: Inlet and outlet flow and pressure curves illustrate the last two cardiac cycles of the simulation for constant pressure (90 mmHg) and impedance outlet boundary conditions. This image was reproduced with the permission of Vignon-Clementel *et al.* [10].

2.3 Embolus particle motion using the modified Maxey-Riley equation

The embolus is assumed to be a spherical particle (with a first-order approximation) with a nominal density of 1100.0 kg/m^3. The motion of this particle within the vasculature is modeled using a modified form of the Maxey-Riley equation, derived from superposition of the steady and unsteady forces on the particle arising from the background flow as well as the disturbed flow around the particle. The Maxey-Riley equation is fundamental to all particle dynamics studies. However, the equation is often modified to account for particle-wall and particle-particle interactions, depending on the complexity of the simulation framework. This section reviews the development of the modified form of Maxey-Riley equation, starting with its original form and discussing the modifications in further sections [3].

Maxey and Riley [3] present the force on the sphere in terms of the body force, and the integral of the traction vector over the surface of the sphere. They split the velocity field into an undisturbed component and a component disturbed due to the presence of the sphere. A general equation was then presented by Maxey *et al.* under the following assumptions: incompressible flow, no-slip boundary condition at the surface of the sphere, small size of the sphere compared to the characteristic length scale such that far-field fluid velocity is unaffected by the presence of the sphere, no particle-boundary interaction (the distance between the sphere and the nearest boundary is much greater than the radius of the particles), and no particle-particle interaction (the distance between any two particles is much greater than the radius of the particles). The equation is shown below, where the specific significance of each term is indicated in Eq. (5). The Stokes' Viscous Drag term is the most significant. The Basset History and the Added Mass terms result from retaining the time derivative and are often negligible. The Buoyancy term is significant only if the difference in densities of the fluid and the particle is considerable [3].

$$m_\rho \frac{dV_i}{dt} = \overbrace{(m_\rho - m_F)g_i}^{Buoyancy} + \overbrace{m_F \frac{Du_i}{Dt}\Big|_{Y(t)}}^{Pressure\ Gradient} - \overbrace{\frac{1}{2}m_F \frac{d}{dt}[V_i(t) - u_i(Y(t),t)] - \frac{1}{10}a^2\nabla^2 u_i\Big|_{Y(t)}]}^{Added\ Mass}$$
$$\underbrace{-6\pi a\mu[V_i(t) - u_i(Y(t),t) - \frac{1}{6}a^2\nabla^2 u_i\Big|_{Y(t)}]}_{Viscous\ Stokes'\ Drag} \underbrace{- 6\pi a^2\mu \int_0^t d\tau \left(\frac{d/d\tau V_i(t) - u_i(Y(t),t) - \frac{1}{6}a^2\nabla^2 u_i\Big|_{Y(t)}}{(\pi\nu(t-\tau))^{1/2}} \right)}_{Basset\ History} \quad (5)$$

Although the simulation frameworks in the current studies on emboli transport maintained the spherical shape in accordance with the derivation of Eq. (5) [3], expected plastic and elastic deformations were accounted for in computing coefficients of restitution due to particle wall impacts ([1], which required addition of terms in the original form of Eq. (5). The full form of the particle motion Eq. (5) can be computationally expensive, given the evaluation of the history terms. This term can be neglected to obtain a "**one-way coupled**" fluid-particle interaction (where the reciprocal exchange of momentum from particle to fluid is neglected) by considering the small-particle assumption [6, 7]. A non-dimensionalized form of Eq. (5) can be formulated (refer Mukherjee *et al.* [6]) to obtain a simpler and less computationally-intensive first-order approximation [6] where the parameter $\tau_p = \frac{\rho_p D_p^2}{18\mu_f}$ indicates individual particle response time to the background flow. This parameter is used to define the particle Stokes number as $\frac{\tau_p}{\tau_{characteristic}}$. Since, the relative contribution of the history force terms scales as $\sqrt{\frac{\tau_p}{\tau_{characteristic}}}$, the history force can be neglected for the cases where the particles are small to moderately small in size. These modifications based on the embolus size and density approximations lead to a simpler form of particle-motion equation as given by

the following:

$$m_p \frac{dv_p}{dt} = F_p = \frac{1}{2}\rho_f C_D(\frac{\pi D_p^2}{4})|u - v_p|(u - v_p) + \nu_p(-\nabla p + \nabla \cdot \tau) + \frac{C_a \rho_f \nu_p}{2}[\frac{Du}{Dt} - \frac{dv_p}{dt}] + \mathcal{I}(\mathcal{P}, \mathcal{W})F_{contact} \quad (6)$$

where the last term accounts for the particle wall contact and is significant in the development of a more rigorous particle transport model, as discussed in the next section. Although Maxey *et al.* considered a small particle size compared to the vessel diameter, the particle-fluid or two-way coupled interaction terms become significant for an accurate description as the particle size becomes comparable to vessel diameter. However, accounting for two way coupled interactions is far more computationally expensive than considering one-way coupled interactions. A method for accounting two way interactions is discussed in section 2.4.

2.3.1 Embolus contact with vessel wall

In order to understand the mechanics of embolic occlusion of an artery–which ultimately leads to stroke– the role of detailed particle interactions with the vessel wall cannot be ignored. The last term on the right-hand side of Eq. (6) incorporates this interaction where $\mathcal{I}(\mathcal{P}, \mathcal{W})$ is the indicator function calculated from triangulation of the vessel wall surface [6]. The point of contact kinematics equations of the assumed spherical embolus are employed in form of rolling motion on the vessel wall, which helps to define unique tangent slip vectors contacting the triangle, which are used to define the tangential and normal components of the contact force on the triangle element. The effect of inelastic deformations and energy loss during contact can be incorporated by using restitution coefficient e (as a result of linear momentum balance on the particle) [6], using which the total average normal contact force on the particle can be calculated.
In their previous studies [5, 6] Mukherjee *et al.* resolved the effect of particle collision with a constant restitution coefficient value without incorporating the effect of embolus properties. In their recent work [7], they incorporate a 'soft-contact' model. When the particle surrounded by fluid comes in contact with the wall, a thin viscous lubrication layer increases the pressure loading on the particle, causing it to deform. This leads to added dissipation upon contact, where the effective restitution coefficient (e_{eff}) differs from the typical dry restitution coefficient (e_{dry}). Since the particles swirl around in the tortuous arterial segments, a consistent treatment of the particle wall contact mechanics is important to account for realistic dissipation of energy upon contact. Accounting for the effects of elastohydrodynamic lubrication is relevant since both the embolus and the artery inner wall lining are soft subsrates; presence of a lubrication layer will cause rise in pressure and deformation. In the absence of elastohydrodynamic considerations, purely rigid particles in Stokesian flow conditions will not rebound at low impact velocities giving incorrect velocity predictions. Thus, the soft-contact model accounts for a more realistic combination of material mechanical properties, as well as collision velocities.

2.4 Particle fluid two-way coupling vs. one-way coupling

As discussed in section 2.3, accurate computational modeling of the particle trajectories requires consistent numerical resolution of interaction between the fluid and the particle [6]. While fluid forces on the particle are of greatest consideration, the presence of a particle in the fluid leads to a two-way exchange of momentum locally back to the fluid–referred to as "two-way coupled" or "fully-coupled" fluid-particle interaction. Two-way coupled formulations can be broadly categorized into two types: 1) direct resolution of flow around the particle, and 2) particle interaction with the fluid in the form of momentum sources. Since the second method is more robust in terms of repeatability for a large population of particles, Mukherjee *et al.* in their study on fluid-particle interactions, employed a particle-source type coupling strategy achieved by augmenting the Navier-Stokes equation with momentum source terms where the transfer of momentum is onto the carrier fluid by the particle [6]. The source term for each computational cell is represented by

an averaged sum of net forces applied by all the particles accounted in that cell. The particle sizes were chosen to be in the range of 10-750 μm, such that they were in the small to moderate regime when compared to vessel diameter [6]. For the one-way coupled simulations, the particles were all released at once, as it was assumed that they neither interact with the flow nor with each other. Whereas for the two-way coupling, each trajectory computation was performed separately with an independent flow field solution (the reason this method was considered to be computationally expensive). The significance of two-way coupling was thus demonstrated by the fact that the difference in embolus distribution in carotid bifurcation with and without two-way interactions was found to be 5.3% in the anatomical bifurcation. This affects the predilection of embolic transport to the cerebral arteries, which ultimately affects the dynamics of stroke. An important factor worth mentioning for most of the papers discussed here is that the particle sizes considered are well below the regimes where geometric obstruction will become a significant factor in biasing the particles towards the wider branch or reducing the flow of particles into the narrower branch.

3 Interaction of emboli with vortical flow

Arteries are inherently curved, non-planar, and vary in compliance depending on their particular functional characteristics. This causes local structures to develop in blood flow. The embolus particle interaction with local flow structures plays a significant role in the distribution of particles across a bifurcation, whereby modeling of these anatomical flow variations becomes necessary as these variations result in secondary vortical and swirling flow [6]. Although the scope of this paper is directed to computational studies (since past in-vitro studies on particle transport were found limited in being able to incorporate geometric variation) [1, 6], it was found that including one current bench-top study can highlight the applicability of in-vitro experimentation to obtaining accurate anatomical flow features.

3.1 Experimental study of aortic flow

Gulan *et al.* [2] studied blood flow in an in-vitro model of a human ascending aorta with compliant walls using 3D Particle Tracking Velocimetry (PTV). The complexity in the geometry, the pulsatility, and the non-stationary nature of its boundaries owing to its high distensibility, made this study challenging. The main components in the experimental setup were: Ventricular Assist Device (VAD), laser, reflecting mirrors, a high-speed camera that can record 1.56 seconds at full resolution and a frame rate of 7000 fps. The Ventricular Assist Device, which was used to stimulate the pumping action of the heart, produced 42 heartbeats, each lasting 1.159 s. Each pulse consisted of a systolic, decelerating, and diastolic period. The Stoke's number was stated to be of the order of 0.01 to 0.001, implying very responsive tracer particles. They obtained the velocity field, flux, vorticity, and other Lagrangian and Eulerian properties.

During the systole, the volumetric flux is positive, and the velocity profile at the inlet gradually skews more towards the inner wall. In this phase, the helical pattern of the flow is indistinct. In the dyastolic phase, a bidirectional flow is observed, with a dominant retrograde flow along the inner wall of the aorta. There is an antegrade flow near the outer wall, but it is not as pronounced as the retrograde flow, which substantially affects the helical pattern of the flow. The deceleration phase is characterized by a coherent bi-helical flow due to the combination of antegrade and retrograde flows.

A single-particle dispersion analysis was done, and the results show that particle dispersion is low in the systolic phase, increases in the late systolic, deceleration and early diastolic phase, and peaks mid-diastole. Fig. 3(b) shows the helical pattern of the pathlines at the mid-diastolic phase.

The role of anatomical variations in flow characterization was studied computationally by Mukherjee *et al.* [6] whereby they compared the emboli trajectory between the idealized and the anatomical models. For the idealized model, the particles travel in rectilinear paths up to the bifurcation such that the local flow structures at the bifurcation alone will determine the distribution behavior. In contrast, the particle pathlines for the anatomical model exhibit substantial helical motion prior to approaching the bifurcation, as displayed in Fig. 3(a). Thus, significant differences in how particles are transported across the arteries may be in large part due to helical flow structures.

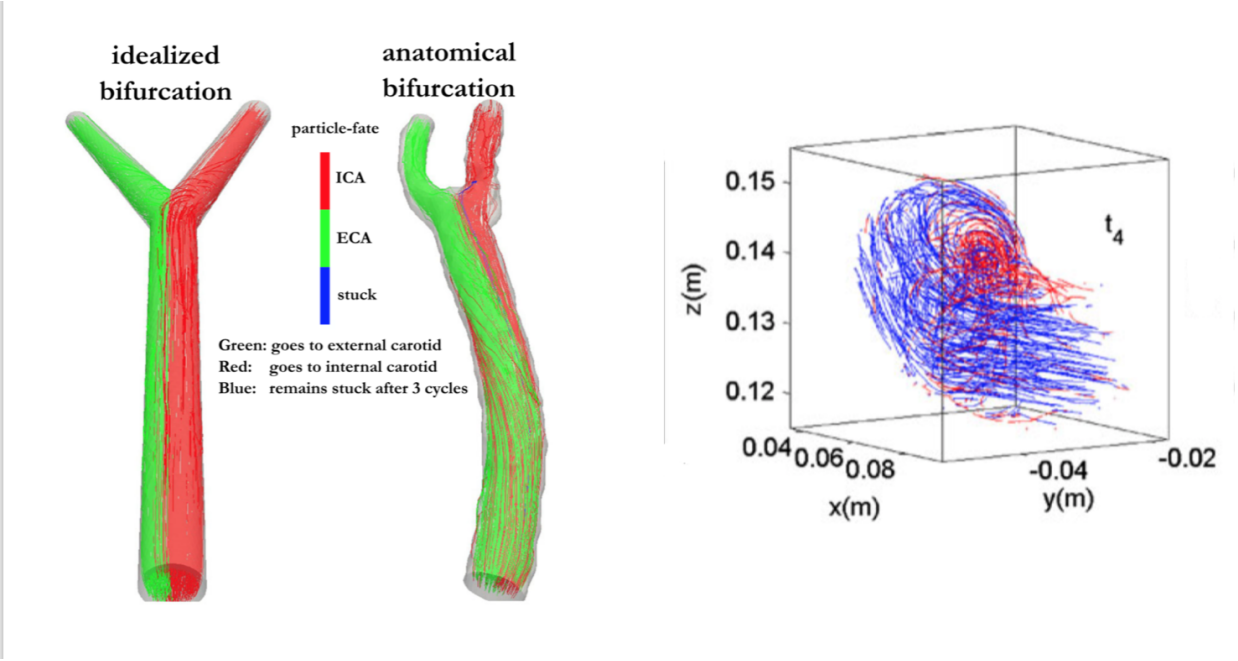

(a) (b)

Figure 3: (a) Particle path lines for 750 μm emboli traveling across the idealised (left), and the anatomical (right) bifurcations–colored by the branch vessel they migrate to across the bifurcation. This figure is reproduced with permission from Mukherjee *et al.* [6] (b) Helical flow in ascending aorta, due to pulsating flow. This figure is reproduced with permission from Gulan *et al.* [2].

4 Conclusions

The literature review primarily aimed to describe the development of particle transport dynamics while considering various parameters influencing the motion of particles. This research finds extensive application in modeling embolus transport, which play a crucial role in cardiovascular diseases. The computational fluid dynamics framework is a powerful tool for modeling variation of embolic transport phenomena with complex geometries and flow structures. The CFD model makes it possible to resolve the particle-fluid interaction that can be described by one-way and two-way coupling. Two-way coupling continues to be an active area of research. The current method of numerical resolution of the two-way interaction by assuming the particle-fluid interactions as momentum sources has a limitation, as it is only applicable for particles of small and moderate diameter and cannot be extended to larger particles [6]. The attractiveness of one-way coupling is based on reasonable computational costs and accuracy. The ability to non-invasively characterize embolus transport is of great utility in the treatment of cardiovascular diseases. Evaluating embolus transport and source–destination relationships over vasculature regions where surgery is to be performed can have implications for treatment or device design. Challenges in the existing computational framework are inapplicable to larger emboli, since the characterization of dynamics of larger emboli potentially occluding the large vessels will require a different, fully resolved, fluid–structure interaction-based approach [7].

References

[1] Ian A Carr, Naohiko Nemoto, Robert S Schwartz, and Shawn C Shadden. Size-dependent predilections of cardiogenic embolic transport. *American Journal of Physiology-Heart and Circulatory Physiology*, 305(5):H732–H739, 2013.

[2] Utku Gülan, Beat Lüthi, Markus Holzner, Alex Liberzon, Arkady Tsinober, and Wolfgang Kinzelbach. Experimental study of aortic flow in the ascending aorta via particle tracking velocimetry. *Experiments in fluids*, 53(5):1469–1485, 2012.

[3] Martin R Maxey and James J Riley. Equation of motion for a small rigid sphere in a nonuniform flow. *The Physics of Fluids*, 26(4):883–889, 1983.

[4] Debanjan Mukherjee, Neel D. Jani, Jared Narvid, , and Shawn C. Shadden. The role of circle of willis anatomy variations in cardio-embolic stroke: a patient-specific simulation based study. *Annals of Biomedical Engineering*, 46(8):1128–1145, 2018.

[5] Debanjan Mukherjee, Neel D. Jani, Kartiga Selvaganesan, Christopher L. Wang, and Shawn C. Shadden. Computational assessment of the relation between embolism source and embolus distribution to the circle of willis for improved understanding of stroke etiology. *Journal of Biomedical Engineering*, 138(081008):1–13, 2016.

[6] Debanjan Mukherjee, Jose Padilla, and Shawn C Shadden. Numerical investigation of fluid–particle interactions for embolic stroke. *Theoretical and Computational Fluid Dynamics*, 30(1-2):23–39, 2016.

[7] Debanjan Mukherjee and Shawn C Shadden. Inertial particle dynamics in large artery flows–implications for modeling arterial embolisms. *Journal of biomechanics*, 52:155–164, 2017.

[8] Mette S Olufsen. Structured tree outflow condition for blood flow in larger systemic arteries. *American journal of physiology-Heart and circulatory physiology*, 276(1):H257–H268, 1999.

[9] Adam Updegrove, Nathan M Wilson, Jameson Merkow, Hongzhi Lan, Alison L Marsden, and Shawn C Shadden. Simvascular: an open source pipeline for cardiovascular simulation. *Annals of biomedical engineering*, 45(3):525–541, 2017.

[10] Irene E Vignon-Clementel, C Alberto Figueroa, Kenneth E Jansen, and Charles A Taylor. Outflow boundary conditions for three-dimensional finite element modeling of blood flow and pressure in arteries. *Computer methods in applied mechanics and engineering*, 195(29-32):3776–3796, 2006.